Materials Advances

ROYAL SOCIETY OF CHEMISTRY

PAPER

View Article Online
View Journal

Cite this: DOI: 10.1039/d5ma01323b

Design and engineering of novel extrusion-cast films from plasticized cellulose acetate filled with mineral fillers for flexible packaging applications

Fatemeh Jahangiri, [ab] Matias Menossi, [ab] Manjusri Misra *[ab] and Amar K. Mohanty *[ab]

Plasticized cellulose acetate (pCA)-based green composite films were fabricated *via* cast film extrusion as sustainable alternatives to solvent-cast processing and conventional petroleum-based plastics for applications in flexible packaging. Cellulose acetate was plasticized with bio-based triacetin (pCTA) or petrochemical triethyl citrate (pCTEC). Green composites were then prepared by incorporating 10 or 15 wt% talc or recycled $CaCO_3$ ($rCaCO_3$) with an optimized amount of Luperox (LUP) used as a compatibilizer. The combined addition of fillers and LUP significantly enhanced the elastic modulus (EM) of all samples, particularly for talc-filled systems. Specifically, EM increased by 126% in pCTA/LUP/15Talc and by 136% in pCTEC/LUP/15Talc compared with pCA. The tensile strength (TS) also improved by 31–40% in talc-filled films, while $rCaCO_3$-filled films showed minimal changes. These enhancements were attributed to improved interfacial adhesion between talc and pCA, promoted by LUP as well as orientation of talc crystallites and polymer chains during cast film extrusion. X-ray diffraction confirmed the higher nucleating efficiency of talc, yielding higher crystallinity values of 75–84% for talc-filled *versus* 66–69% for $rCaCO_3$-filled pCA. Talc-filled films also exhibited superior elongation at break (EB), thermal stability, and barrier performance, with oxygen and water vapor permeability reductions of up to 38% and 72%, respectively. Talc-filled films' higher contact angles (for both water and diiodomethane) and lower surface energy further supported the improved barrier properties. Overall, the synergistic effects of LUP and talc significantly enhanced the mechanical strength, barrier effectiveness, and thermal stability of pCA composites, demonstrating their strong potential as sustainable materials for flexible packaging applications.

Received 13th November 2025,
Accepted 12th April 2026

DOI: 10.1039/d5ma01323b

rsc.li/materials-advances

1. Introduction

Cellulose, the most abundant polysaccharide on Earth,[1] can be converted into cellulose acetate (CA) – a polymer of growing interest for sustainable applications. Moreover, CA is approved by the Food and Drug Administration as GRAS (Generally Recognized as Safe). CA is used in food-related applications such as disposable cutlery and produce wrapping.[2] However, its poor tear strength and limited barrier properties against moisture and gases restrict its broader use. To overcome these limitations, researchers have explored blending CA with other polymers[3] or reinforcing it with fillers to enhance performance.[4]

The number of hydroxyl groups that are substituted by acetyl groups in a single anhydroglucose unit determines the degree of substitution (DS) of the CA. The DS, which can be in the range of 1.7–3.0,[5] is a primary factor that determines the rate of CA's biodegradability. The higher the DS, the lower the biodegradation rate.[6] A higher DS also increases gas permeability by expanding the polymer structure and reducing hydrogen bonding.[7] Thus, more research on low-DS CA is needed, as it offers higher biodegradability rates and gas barrier properties for sustainable packaging applications.

CA's strong dipolar interactions result in a high glass transition temperature (T_g) and a narrow temperature range between melting and decomposition limits its processability.[3] Plasticizers are essential to overcome these challenges and improve CA's processability.[2,8] Glycerol-based plasticizers such as TA and citrate plasticizers such as TEC are well-known additives originating from renewable molecules that are used in the plastic industry as a replacement for phthalate- and dibenzoate-based plasticizers.[9] The typical plasticizer content that is added to CA is 15–35 wt%.[10] For instance, 25% TEC was reported as an optimized amount to plasticize CA with optimal mechanical properties without compromising its structural

[a] *Bioproducts Discovery and Development Centre, Department of Plant Agriculture, Crop Science Building, University of Guelph, 50 Stone Road East, Guelph, Ontario, Canada. E-mail: ffjahangi@uoguelph.ca, mmenossi@uoguelph.ca, mmisra@uoguelph.ca, mohanty@uoguelph.ca*

[b] *Department of Interdisciplinary Engineering, College of Engineering, THRN Building, University of Guelph, Guelph, Ontario, N1G 2W1, Canada*

integrity.[5] Moreover, plasticization of CA with 25% TA results in continuous strands without any breakage during processing.[11] It has been reported that CA plasticized with $\geq$25% plasticizer was needed for high impact resistance at room temperature, marking it a critical threshold for toughness. Beyond this level, miscibility issues caused inconsistent yield stress behavior,[12,13] suggesting 25% as the optimal plasticizer content for CA.

Talc, a hydrous magnesium silicate ($Mg_3Si_4O_{10}(OH)_2$), is certified safe for specific food use according to a Canadian government report[14] and is widely used as a reinforcement filler in a polymeric matrix to improve the mechanical and barrier properties. $CaCO_3$ is an abundant mineral commonly found in limestone[15] and it can be recycled from sea shell waste[16] or paper sludge[17] supporting circular economy efforts. Composite performance depends heavily on effective stress transfer at the fiber–matrix interface, making interfacial bonding a key focus in composite design.[18] Thus, compatibilizing agents, such as organic peroxide compounds,[19] are commonly used to enhance interfacial compatibility. During reactive extrusion, peroxides can trigger chain scission, branching, and crosslinking, improving adhesion and stress transfer. Similar effects can occur in polymer-filler systems. However, peroxide content must be optimized, as excess can cause phase separation.[20]

In our previous work,[21] the effect of different inorganic fillers at 10% wt (talc, $CaCO_3$, kaolin clay) and a natural fiber (microcrystalline cellulose) in pCA-based composites prepared by melt extrusion and injection molding was studied for rigid packaging applications. Overall, pCA-filled talc composites showed superior mechanical and barrier properties compared with pCA-filled $CaCO_3$, while in terms of thermal properties the T_{onset} was higher for pCA-filled $CaCO_3$ (by 16 °C) *versus* pCA-filled talc. The pCA-filled talc improved the elastic modulus (EM) by 30% compared with neat pCA, while the EM of pCA-filled $CaCO_3$ remained almost unchanged. Similar to CA's increased thermal stability induced by fillers in the previous study, especially $CaCO_3$, the CA-$CaCO_3$ nanocomposites exhibited a growth in the CA's thermal stability by 30 °C compared to neat CA.[22] These hybrid nanocomposites were fabricated through bubbling CO_2 into the mixture of CA and $Ca(OH)_2$ solution. The development of CA-based composites filled with talc, in particular, or $CaCO_3$ is very limited in the available literature to the best of our knowledge. However, there are studies that compared these fillers in other polymeric matrices such as polypropylene (PP)[23,24] or polyvinyl chloride (PVC)[25] which reported the same trends. For example, PP-filled 30 wt% talc-rich hybrid composites prepared by melt extrusion followed by injection molding demonstrated superior tensile and flexural strength as well as higher modulus, whereas hybrid composites containing higher proportions of $CaCO_3$ exhibited greater toughness and deformability.[23] A notable hybridization effect occurred when half of the talc content was substituted with $CaCO_3$ (PP : talc : $CaCO_3$ 70 : 15 : 15), resulting in a more pronounced increase in flexural and impact strength. Similarly, hybrid PP/talc/$CaCO_3$ (at 5 wt% filler) composites prepared by melt blending using a hot press, resulted in higher elastic and flexural moduli and better thermal stability than single-filler PP at similar total loading, again with improved toughness *versus* talc alone.[24] However, at a higher filler loading (more than 5 wt%), the mechanical properties were reduced due to poor filler–matrix adhesion. In another study, talc-rich PVC composites prepared by compression molding, showed higher stiffness (flexural modulus) and the lowest impact strength, while $CaCO_3$-rich PVC composites showed optimum properties in terms of impact resistance and flexural modulus. The hybrid filler composites exhibited a gradual increase in impact strength, while the flexural modulus, flexural strength, elastic modulus, and tensile strength (TS) reduced with increasing $CaCO_3$ content. The authors reported that the best stiffness–toughness balance was achieved by combining 20 phr $CaCO_3$ and 10 phr talc in PVC-based composites.[25]

Most studies on CA-based bioplastic films employ solution casting,[26–29] though hot-melt cast extrusion remains the industry standard for plastic film production.[30] For instance, cellulose nanofibril (CNF) reinforced CA films produced by solvent casting, plasticized with 30 wt% TA and TEC, showed 38% and 65% improvements in TS and EM, respectively, at 5 phr CNF, though higher loading reduced performance due to agglomeration.[27] Similarly, nanocrystalline CA films with 0.8 wt% graphene oxide achieved ~62% higher TS, ~64% higher EM and ~47% lower water vapor permeability (WVP), while higher loadings worsened barrier properties.[31] El-Rehim *et al.*[32] reported that adding 5 wt% clay to pCA films plasticized with polyethylene glycol (PEG) (16 wt%) decreased oxygen and water vapor transmission while enhancing TS and elongation at break (EB), underscoring their packaging potential. Shlush *et al.*[30] showed that solution casting and hot-melt extrusion of ethyl cellulose with myvacet and glycerol produced films with distinct properties: extrusion yielded smoother, stronger films (TS ~ 5–10 MPa, EB ~ 10–60%) and slightly lower T_g and T_m. Myvacet-plasticized ethyl cellulose films processed by extrusion also showed reduced T_g and T_m, improved mechanical properties, WVTR of 76–109 g m^{-2} day, and hydrophilicity suitable for fresh produce.[33] Extruded pCA/anionic clay films with 5 wt% filler showed 12.5% higher EM but 77.7% lower EB due to filler-induced brittleness, yet preserved pomegranate quality during storage.[34] Similarly, pCA/cellulose nanowhisker composites (5 wt%) improved TS and EM by 100% and 300%, though EB dropped 87%.[35] Melt-extruded pCA/montmorillonite nanocomposites plasticized with TEC and loaded with antimicrobial agents exhibited reduced TS and EM, and a 150% increase in WVP.[36] Finally, thermoplastic starch (TPS)–CA films produced using a catalyst showed enhanced hydrophobicity, TS (by 146%), EB, and toughness compared to neat TPS, indicating their potential for food packaging applications.[37]

In pursuit of sustainable packaging solutions, we hypothesized that the synergistic use of suitable plasticizers and inorganic fillers, coupled with reactive compatibilization *via* LUP, could substantially improve the processability, mechanical performance, and barrier properties of CA. Accordingly, the objective of this study is to establish structure–property relationships in pCA composite films by systematically evaluating the effects of the plasticizer type (bio-based TA and petro-based TEC) and filler type (talc and recycled $CaCO_3$) on the final performance of developed composite films. The main distinction of this work in

comparison to our previous work[21] lies in the development of uniform, defect free cast films derived from cellulose acetate-based composites through an industrially relevant melt-extrusion processing approach for flexible packaging applications, unlike our previous work in which pCA-composites were processed through injection molding for rigid packaging applications. Furthermore, unlike prior CA processing studies in the literature, this work integrates (1) renewable and petro-based plasticizers (TA and TEC), (2) inorganic fillers (talc and recycled $CaCO_3$), and (3) peroxide-driven interfacial compatibilization, and systematically links these factors to structure–property relationships encompassing rheological, crystallinity, mechanical, morphological, contact angle and surface energy as well as barrier properties designed for flexible packaging applications.

2. Experimental

2.1. Materials

Cellulose diacetate (CA) (based on the technical datasheet: CAS 9004-35-7, RTW grade, approximate purity 100 wt%, specific gravity 1.31–1.32 g cm^{-3}, T_m 230–250 °C, T_d 304 °C, degree of polymerization 185, combined acetic acid 52.8%, free acidity 0.01%, degree of substitution DS 2.26, wood pulp nature and molecular weight (MW) of 91098.72 g mol^{-1}) was sourced from Sichuan Push Acetati Co., Ltd. The MW and DS calculations are provided in the supplementary information (SI). Food-grade bio-based TA was supplied by Wuhan Golden Wing Industry, and TEC was purchased from Sigma-Aldrich. Luperox DHBP 101 (LUP), with 10.25–10.47% active oxygen was purchased from Arkema. Jetfine 3CC talc (CAS 14807-96-6) and ReMined recycled calcium carbonate ($rCaCO_3$) powder were provided by Imerys, USA. Glycerol (ACS reagent, ≥ 99.5%) was purchased from Sigma-Aldrich. All materials were used as received.

2.2. Plasticization of cellulose acetate

CA powder was dried in an oven at 80 °C. The moisture content of CA was measured using a Sartorius MA37 moisture analyzer before initiating plasticization to be <1%. For plasticization, the CA powder was mechanically blended with 25% plasticizer (TEC or TA), and then left to rest at room temperature for 4 hours. The term ''plasticized CA'' (pCA) refers to CA powder containing 25% plasticizer. When TA is used as the plasticizer, the material is labeled pCTA, whereas pCTEC designates the sample plasticized with TEC.

2.3. Melt extrusion of pCA and composites

Depending on the chosen ratios of pCA, organic peroxide (LUP) and fillers, each formulation was produced using a Micro-27 co-rotating twin-screw extruder (Leistritz Advanced Technologies Corporation, USA). The extruder was operated at temperatures of 160 °C in zone 1 and 180 °C in the remaining zones, with a screw speed of 100 rpm and a feed rate of 6–7 kg h^{-1}. Before extrusion, the required amounts of all components were accurately weighed and manually premixed in zip-lock bags, then loaded into the extruder hopper. After processing, the extruded materials were cooled in a water bath, pelletized, dried overnight at 70 °C, and finally kept in aluminum bags for storage. A complete list of the formulations is provided in Table 1.

2.4. Extrusion casting of pCA and pCA-based composite films

The dried pellets made by melt extrusion in Section 2.3 were cast into films using a cast film extruder (Microtruder RCP-0625, Randcastle, USA, 24 : 1-L : D) (Fig. 1) with a 1.25″ single screw, a lip die and chill rollers. Each composition was processed at a specific temperature, as summarized in Table 2. The lip die gap was adjusted to produce films with a thickness of < 0.25 mm.

2.5. Mechanical properties

The mechanical properties of the cast films were studied in the machine direction per ASTM D882-18 using a universal testing machine (Instron 3382, Massachusetts, USA) equipped with Bluehill software, at 25 ± 2 °C and 50% relative humidity with a 5 kN load cell. The crosshead speed, gauge length and sample dimensions were selected based on the anticipated EB% per ASTM D882-18. Each sample was tested with ten replicates.

2.6. Rheological properties

Rheological measurements were carried out at 200 °C, the average temperature used during cast film processing, using a strain-controlled AntonPaar MCR-302 rheometer. To characterize the frequency-dependent behavior of the pellet

Table 1 pCA-based formulations prepared in the present study with either TA or TEC with/without LUP and fillers. pCA: plasticized cellulose acetate, TEC: triethyl citrate, TA: triacetin, LUP: luperox, $rCaCO_3$: recycled calcium carbonate

Formulation	Sample ID	CA (wt%)	Plasticizer (wt%)	Luperox (phr)	Filler (wt%)
pCA (25%TA)	pCTA	75.00	25.00	—	—
pCA (25%TEC)	pCTEC	75.00	25.00	—	—
pCA (25%TA) + 0.01Luperox	pCTA/0.01LUP	75.00	25.00	0.01	—
pCA (25%TEC) + 0.01 Luperox	pCTEC/0.01LUP	75.00	25.00	0.01	—
pCA (25%TA) + 0.01 Luperox + 10%Talc	pCTA/0.01LUP/10Talc	67.50	22.50	0.01	10
pCA (25%TEC) + 0.01 Luperox + 10%Talc	pCTEC/0.01LUP/10Talc	67.50	22.50	0.01	10
pCA (25%TA) + 0.01 Luperox + 15%Talc	pCTA/0.01LUP/15Talc	63.75	21.25	0.01	15
pCA (25%TEC) + 0.01 Luperox + 15%Talc	pCTEC/0.01LUP/15Talc	63.75	21.25	0.01	15
pCA (25%TA) + 0.01 Luperox + 10%$rCaCO_3$	pCTA/0.01LUP/10$rCaCO_3$	67.50	22.50	0.01	10
pCA (25%TEC) + 0.01 Luperox + 10%$rCaCO_3$	pCTEC/0.01LUP/10$rCaCO_3$	67.50	22.50	0.01	10
pCA (25%TA) + 0.01 Luperox + 15%$rCaCO_3$	pCTA/0.01LUP/15$rCaCO_3$	63.75	21.25	0.01	15
pCA (25%TA) + 0.01 Luperox + 15%$rCaCO_3$	pCTEC/0.01LUP/15$rCaCO_3$	63.75	21.25	0.01	15

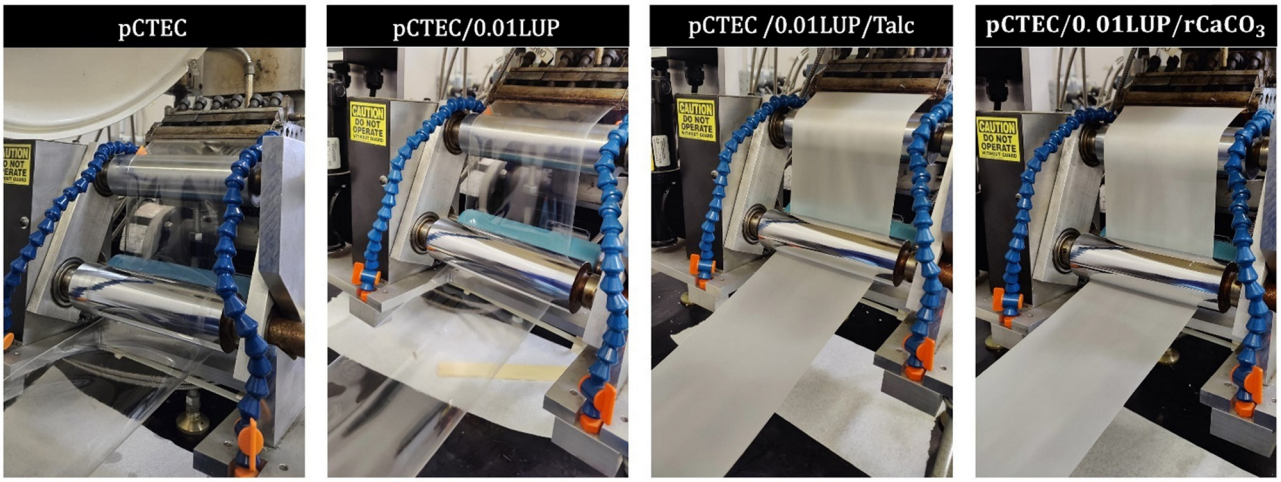

Fig. 1 The neat pCTEC, pCTEC/0.01LUP and pCTEC/0.01LUP/10 or 15 Talc and pCTEC/0.01LUP/10 or 15 $rCaCO_3$ films prepared by cast film extrusion. The films using TA or TEC seem similar in appearance, so only pCTEC-based films are shown for simplicity. pCTEC: plasticized cellulose acetate with triethyl citrate, TEC: triethyl citrate, and LUP: luperox.

Table 2 Conditions in the cast film extruder used for each composition in this study. pCTEC: plasticized cellulose acetate with triethyl citrate, pCTA: plasticized cellulose acetate with triacetin, TEC: triethyl citrate, TA: triacetin, LUP: luperox, and $rCaCO_3$: recycled calcium carbonate

Sample ID	Temperature (°C) in zone 1, zone 2, zone 3, zone 4, die	Screw rotation speed (rpm)	Take-up roller speed (rpm)
pCTA	195	40	20
pCTEC	200	40	20
pCTA/0.01LUP	210	40	25
pCTEC/0.01LUP	210	40	25
pCTA/0.01LUP/10 or 15 Talc	200	40	22
pCTEC/0.01LUP/10 or 15 Talc	200	40	22
pCTA/0.01LUP/10 or 15 $rCaCO_3$	195	40	22
pCTEC/0.01LUP/10 or 15 $rCaCO_3$	195	40	22

samples, tests were performed in dynamic oscillation mode with a 25 mm parallel-plate fixture and a 1 mm measurement gap, all under a nitrogen atmosphere. The complex viscosity along with the storage and loss moduli were quantified across a frequency range of 0.01–100 s^{-1} while maintaining a constant strain of 0.1%. The results of rheological analysis are presented in Fig. S1 and S2.

2.7. X-ray diffraction (XRD)

The crystallinity percentage of the samples was determined through powder X-ray diffraction (XRD), employing a PANalytical Empyrean diffractometer (CuKα, λ = 1.5418 Å, 45 kV, 40 mA, 2θ range 5–60°). Data acquisition and analysis were carried out using a Data Collector and HighScore Plus (version 4.1) software. Crystallinity was calculated using OriginPro 2025.b software and eqn (1), which compares the area under the crystalline peaks (A_C) to the total diffractogram area (A_T).[38]

$$X_c^{XRD}(\%) = \frac{A_C}{A_T} \times 100 \quad (1)$$

2.8. Thermogravimetric analysis (TGA)

The thermal stability of samples was analyzed using a Q500 analyzer (TA Instruments, Delaware). Each sample (15–20 mg) was subjected to heating at a rate of 10 °C min^{-1} from 25 °C to 600 °C under nitrogen (N_2) gas (purging flow of 40 mL min^{-1} and balancing flow of 60 mL min^{-1}). Derivative TGA (DTGA) curves were used to determine the temperatures at which peak degradation occurred.

2.9. Water vapor absorption (WVA)

The hydrophilicity of the two neat pCA formulations (pCTA and pCTEC) was assessed through water vapor absorption (WVA) testing following the methodology described by Menossi *et al.*[39] Briefly, square specimens (1 × 1 cm^2) were cut and oven-dried at 40 °C for 48 h to remove residual moisture. The initial dry mass (M_i) of each specimen was recorded prior to exposure. Then, the samples were placed in hermetic containers maintained at 25 °C under controlled relative humidity (RH) conditions of 60% and 90%, in accordance with ASTM D5032-19. The desired RH levels were achieved using water–glycerin solutions and verified with a hygrometer (TempPro TP50).

The mass of each specimen was monitored at regular intervals over a 48-h period. The percentage of water vapor absorption was calculated using eqn (2).

$$WVA(\%) = \frac{(M_t - M_i)}{M_i} \times 100 \quad (2)$$

In this study, M_t is the mass of the specimen at a given time (t). All measurements were performed in triplicate. The equilibrium water vapor absorption (WVA_{eq}) was determined as the WVA values reached equilibrium and is reported as the mean ± standard deviation. Each WVA_{eq} value for 60 and 90% RH is provided in Table S1.

2.10. Barrier properties

WVP was determined using a Permatran-W 3/33 analyzer (Mocon, USA) at 90 ± 5% relative humidity (RH) and 37.8 °C per ASTM F1249. The cast film samples (5 cm^2) were mounted between two aluminum frames, and then placed in the dual-chamber module. Highly pure N_2 gas was introduced at 100 cm^3 min^{-1} flow rate. During the test, water vapor that permeated through the sample was transported by the N_2 stream to the sensor, enabling quantification of WVP. For OP analysis, samples with similar dimensions were tested using a Mocon OX-TRAN 2/21 analyzer (USA) at 0%RH and 25 ± 2 °C per ASTM D3985. During testing, a 10 cm^3 min^{-1} flow of N_2 transported the diffused oxygen molecules from the film to the sensor, which then served as the basis for calculating the OP. Experiments were performed in duplicate.

2.11. Attenuated total reflection Fourier-transform infrared (ATR-FTIR) spectroscopy

FTIR spectroscopy was used to study the samples' chemical structures and main functional groups, in the ATR mode, with a Nicolet Summit X instrument (Thermo Scientific). Spectral data were collected in the range of 600 to 4000 cm^{-1}, 4 cm^{-1} resolution, and 256 scans.

2.12. Scanning electron microscopy (SEM)

The microstructures of talc and $rCaCO_3$ powders were studied using SEM (Thermo Fisher Scientific, Quanta FEG 250) at 20 kv. The cast films were studied through SEM (Phenom World BV, Netherlands) at 10 kV. All samples were sputter-coated with gold prior to SEM analysis. The cast film samples were placed in liquid N_2. After ~5 min, samples were cryo-fractured manually to study the cross-sections.

2.13. Contact angle and surface energy

To evaluate the water and diiodomethane contact angles of the cast film samples, a Rame-hart standard goniometer (260-U1, USA) with a high-speed digital camera, 0° stage angle, ±0.01° resolution and ±0.1° accuracy. Films were trimmed into 2 × 2 cm^2 sections and positioned on the sample holder. Using a glass syringe, 5 μL droplets of either water or diiodomethane were placed on the surface of the sample and left undisturbed for approximately 10 seconds. The contact angles were recorded using DROP image advanced software. Each test was repeated in triplicate. Based on the measured contact angles, the surface tension of the cast films was calculated using Young's equation (eqn (3)):[40]

$$\gamma_s = \gamma_{sl} + \gamma_l \cos\theta \quad (3)$$

where γ_s and γ_l refer to the equilibrium surface tensions at solid–vapor and liquid–vapor interfaces, respectively, while γ_{sl} is attributed to the interfacial tension of the liquid and solid phases and θ is the contact angle. The Owens–Wendt–Rabel–Kaelble (OWRK) model extends this concept by applying a geometric mean approach to separate the surface tension into dispersive and polar forces (Table 3). Alternatively, when identical intermolecular forces exist at the interface, the harmonic-mean equation applies. We measured the contact angle of cast films using a geometric- and harmonic-mean[40] and the surface tension was computed using DROP image advanced software.

Table 3 Surface tension (γ) and polar (γ^p) and dispersive (γ^d) components (mN m^{-1}) for water and diiodomethane

Liquid	γ	γ^p	γ^d
Water	72.8	51.0	21.8
Diiodomethane	50.8	0.0	50.8

3. Results and discussion

3.1. Mechanical properties

Mechanical properties (EM, TS, EB%) play a critical role in the functionality and longevity of packaging films. We evaluated the influence of a bio- and a petro-based plasticizer (TA and TEC) along with $rCaCO_3$ and talc fillers on the pCA matrix (Fig. 2). The mechanical properties depended on the miscibility of the plasticizer with CA and filler dispersion in the pCA matrix and their interactions.

3.1.1. Influence of organic peroxide on the pCA-based matrix. The neat pCTA and pCTEC showed almost similar mechanical properties (Fig. 2). The TS, EM and EB% for pCTA were 42.74 MPa, 1.79 GPa, 30.2%, respectively while these parameters for pCTEC were 42.15 MPa, 1.85 GPa, 29.9%, respectively. Overall, the pCA neat films developed here showed superior mechanical performance compared to those reported in the literature. For example, the pCA film fabricated through extrusion showed an EM of 1.12 ± 0.03 GPa and an EB% of 23.8 ± 3%.[34] Similarly, cellulose acetate butyrate (CAB)/20%TEC films were fabricated through a twin-screw extruder showing an EM of 0.79 GPa ± 0.11, a TS of 20 ± 1.62 MPa and an EB% of 18.3 ± 5.1%.[36] The differences in the mechanical properties reported in the literature *versus* this study, can be due to the differences in the plasticizer amount and type, processing temperature, DS of CA used and the type of substituent.

We previously optimized the level of LUP (0.01 phr) added to the pCA to achieve well-balanced mechanical properties.[21] Addition of LUP to the pCTEC matrix resulted in higher TS and EM, which can be due to the crosslinking effect of LUP, which was further confirmed through rheological analysis showing higher complex viscosity after addition of luperox into the pCA matrix (Fig. S1). Peroxide compounds function as a crosslinking agent, thus can improve the mechanical integrity.[41] Specifically, for pCTEC/0.01LUP, the TS and EM increased by ~15% and ~44%, respectively, compared to the neat pCTEC film. In the case of pCTA/0.01LUP, the TS remained almost unchanged after the addition of LUP, while the EM increased by ~31%, compared with the neat pCTA film. The EM indicates the stiffness of the matrix which is mainly controlled by the composition rather than the reactive extrusion reactions. Similarly, addition of 0.02 phr LUP to a ternary blend of polylactic acid (PLA)/polybutylene succinate (PBS)/polybutylene adipate terephthalate (PBAT), resulted in an increased EM and TS.[42]

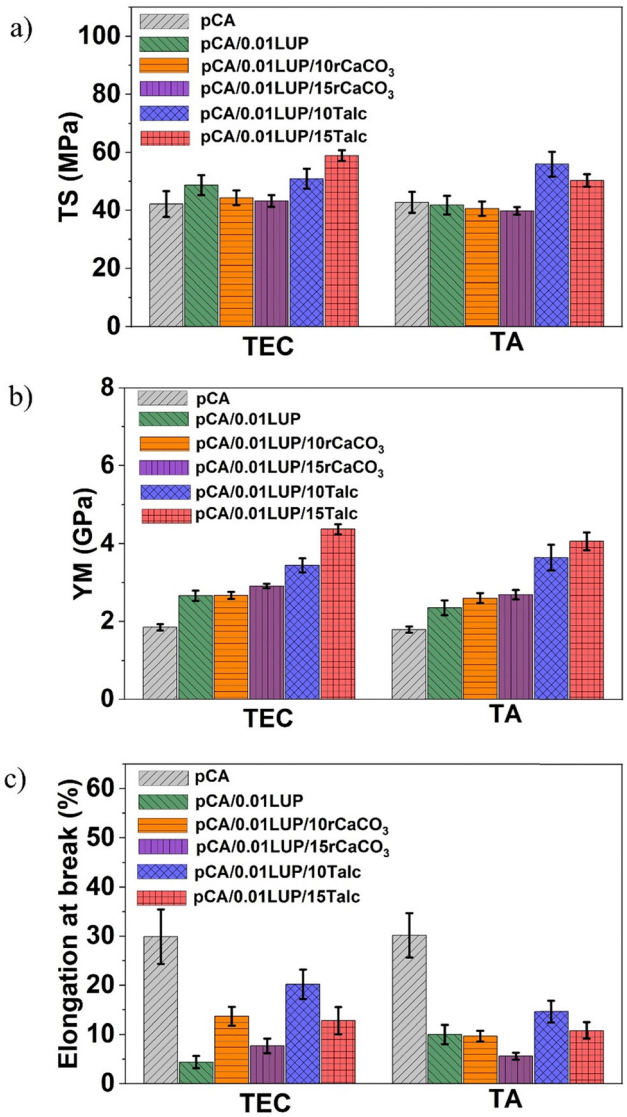

Fig. 2 Mechanical properties of the neat pCA films and pCA-based composite films. (a) Tensile strength (TS), (b) Young's or elastic modulus (EM), and (c) elongation at break (EB%). The combined addition of LUP and fillers increased the EM compared with neat pCA films. The TS remained almost unchanged after the addition of $rCaCO_3$ and LUP, while there was a significant increase after the addition of talc and LUP and finally, the EB% experienced a dramatic reduction across all samples. pCA: plasticized cellulose acetate, TEC: triethyl citrate, TA: triacetin, LUP: luperox, and $rCaCO_3$: recycled calcium carbonate.

In another study, addition of only 0.025 wt% peroxide to a binary blend of polyethylene (PE)/PP, increased the TS significantly due to increased crosslinking.[43]

EB% decreased markedly after peroxide addition, with the EB% reduced in pCTEC/0.01LUP by 85% and 67% for pCTA/0.01LUP, consistent with chain mobility restrictions in crosslinked systems and improved complex viscosity observed in rheological properties (Fig. S1). Liu *et al.*[44] reported that crosslinking in low-density polyethylene (LDPE) involves chemical and physical junctions as well as permanent entanglements. During cooling from melt in cast film extrusion, these junctions restrict elongation by limiting segment mobility and reducing chain slippage, leading to lower EB%. The amount of peroxide strongly influences this trade-off: small additions (0.01 phr in this study) improve TS and EM but reduce flexibility, while higher levels can cause excessive crosslinking and severe EB% loss. For example, 0.05 phr peroxide in a blend of pCA/PBAT, resulted in a higher TS and lower EB%, due to the formation of crosslinked structure.[19] While, in a PE/PP binary blend, Gonzalez *et al.*[43] added 0.025 and 0.05 wt% peroxide and observed higher EB% compared with a neat blend but higher loadings led to sharp declines in EB% as a result of more restrictions caused by crosslinking against the sliding of polymer chains.[43] This further highlights the critical importance of the amount of peroxide compound that is added to a polymeric matrix.

3.1.2. Influence of talc and $rCaCO_3$ fillers on the pCA-based matrix. Overall, the pCA-based composite films developed here showed superior mechanical performance compared to those reported in the literature. For example, pCA-filled layered double hydroxide showed an EM of 1.26 ± 0.07 GPa and an EB% of 5.3 ± 0.7% due to filler-induced discontinuities.[34] In this study, addition of 10 wt% and 15 wt% $rCaCO_3$ or talc into the pCTA or pCTEC matrix showed almost similar trends in TS, EM and EB% compared with pCTEC- and pCTA neat films (Fig. 2). Addition of fillers and further increasing the filler content from 10 wt% to 15 wt%, consistently raised EM across all samples, compared with neat pCTA and pCTEC films due to filler stiffness and restricted chain mobility.[45] This effect was more pronounced in talc composites, particularly pCTA/0.01LUP/15Talc and pCTEC/0.01LUP/15Talc, where the EM increased by 126% and 136%, respectively. Improved interfacial adhesion with talc, aided by 0.01 phr LUP, likely explains this enhancement, which was also confirmed through rheological analysis showing lower complex viscosity with the combined addition of LUP and talc into pCA compared to only talc-filled pCA (Fig. S1). The same observation was reported by Zhu *et al.*,[45] where increasing the silica content in the polystyrene and LDPE increased the EM. Comparable effects of LUP compatibilization were reported for PP–hemp composites.[46]

The TS remained almost unchanged for $rCaCO_3$-filled films compared with neat pCA films, and even slightly declined in pCTA/0.01LUP/$rCaCO_3$ due to filler agglomeration which restricted the effective stress transfer from polymer to the filler. A similar reduction in TS was observed in the case of talc–PBAT composite films,[14] as well as Biochar-PBAT composite films.[47] In contrast, talc-filled films showed significant TS improvements: 40% in pCTEC/0.01LUP/15Talc and 31% in pCTA/0.01LUP/10Talc *versus* pCTEC and pCTA films, respectively. This improvement arises from better dispersion of talc in the presence of LUP, as supported by SEM observations as well as lower viscosity observed in rheological analysis (Fig. S1). Similar results were reported in TiO_2-filled PBAT/thermoplastic starch films[48] or TiO_2-filled starch films.[49] The increase in talc level (from 10 to 15 wt%) exhibited a continued increase in TS for pCTEC-based composites, while the reverse was observed for pCTA-based composites. This is consistent with reports that filler agglomeration and poor interfacial adhesion between filler and polymer initiate crack

propagation resulting in composite failure.[50] It was reported previously that strain-induced crystallization upon stretching the PBSA-filled talc[51] or PBAT-filled talc[14] positively affected the mechanical properties of the films when compared to unstretched films. This can be another reason behind the improvement in TS and EM of the present study, in which orientation of talc crystallites and polymer chains along the draw direction during cast film extrusion processing might occur. However, to verify this phenomenon one needs to compare the film properties in this study with unstretched films.

The improved TS and EM of talc-filled films also correlate with the improved crystallinity after talc addition to the pCA matrix in this study, which is discussed in Section 3.2. Similar observations were reported for PBSA-filled talc[51] and PBAT-filled talc composites.[14] The compatibilization effect of LUP was more effective in talc-filled films rather than in $rCaCO_3$-filled films. This is also evident when comparing the SEM images of talc-filled films with $rCaCO_3$-filled films, which will be further discussed in terms of the SEM analysis (Section 3.3). Talc, due to its platelet-like structure, facilitates more effective stress transfer than spherical or other particle shaped fillers.[51] Because of its platy morphology, talc tends to align with the direction of polymer flow during processing. This shape gives platy fillers a high aspect ratio, which improves their wettability by the polymer matrix. Improved wettability reduces the formation of microvoids and enhances the interfacial contact between the filler and the matrix. As a result, the stronger filler–matrix interaction enables more efficient transfer of stress from the polymer matrix to the talc particles during external loading.[23] Similarly, the PP–hemp bast fiber using LUP as a compatibilizer, showed a 40% increase in TS compared with neat PP.[46]

EB% decreased notably in all filler-loaded films, reflecting reduced chain mobility and increased crystallinity. The lowest values were found for $rCaCO_3$ composites (7.7% for pCTEC/0.01LUP/15$rCaCO_3$ and 5.6% for pCTA/0.01LUP/15$rCaCO_3$), which also showed phase separation and agglomeration in SEM images due to the poor adhesion of filler and polymer matrix. A similar decrease in EB% was reported in a previous study due to an increase in the film crystallinity upon talc addition.[51] The highest EB% among all composites, in this study, was obtained from pCTA/0.01LUP/10Talc (14.6%) and pCTEC/0.01LUP/10Talc (20.2%), which indicate a better filler dispersion in the presence of LUP as a compatibilizing agent compared to those composites with $rCaCO_3$. Conversely, stronger chemical cross-links induced by LUP enhanced intermolecular forces, increasing TS,[44] which was particularly evident in pCA-talc composites.

In summary, the combined addition of LUP and fillers (talc or $rCaCO_3$) increased the EM compared with pCA films. The TS remained almost unchanged after the co-addition of $rCaCO_3$ and LUP, while talc increased the TS significantly. Finally, EB% experienced a drastic decrease after adding LUP and either $rCaCO_3$ or talc into the pCA matrix.

3.2. X-ray diffraction (XRD)

Fig. 3(a–f) show the XRD patterns of talc, $rCaCO_3$, pCA, and their composite films. $rCaCO_3$ powder (Fig. 3a) exhibited sharp peaks of the calcite phase at 2θ = 23.0° (012), 29.4° (104), 35.9° (110), 39.4° (113), 43.2° (202), 47.5° (018), 48.5° (116), and 57.4 (122).[52,53] Talc powder (Fig. 3b) displayed distinct diffraction at 2θ = 9.8°, 19.5°, 29.1°, 38.9°, and 49.1°, corresponding to the (002), (110), (006), (132), and (060) crystallographic planes, respectively.[51]

Neat pCTA and pCTEC (Fig. 3c and e), with or without LUP, showed patterns typical of semi-crystalline polymers, characterized by a van der Waals broad amorphous halo at $2\theta \approx 20°$ and a weaker low van der Waals halo feature near $2\theta \approx 10°$. Another distinct peak at approximately $2\theta \approx 8°$ reflects structural disorder caused by acetylation, which disrupts cellulose microfibril packing and increases interfibrillar spacing. Similar diffraction features were reported by de Freitas *et al.*[54] in CA with a DS of 2.29.

Incorporation of $rCaCO_3$ introduced its characteristic peaks at 29.4°, 47.5°, and 48.5° (Fig. 3c and e), with intensity increasing at 10–15% loading. This suggests enhanced crystallinity and a transition from an initially amorphous halo to more semi-crystalline and ordered domains. Similar findings were reported by Menossi *et al.*[40] for a wollastonite-filled PBAT matrix. It is important to note that as more $rCaCO_3$ is added, the relative proportion of pCA (TA- or TEC-plasticized) decreases, thereby lowering peak intensities associated with pCA (TA- or TEC-plasticized) in the composite due to the reduced presence of the polymer phase.[55]

Similar to $rCaCO_3$-filled films, talc-filled films showed their characteristic reflections (Fig. 3d and f), with intensity increasing at 10–15% loading, indicating improved crystalline organization. Furthermore, a slight shift of the peaks toward lower 2θ values was observed in the pCTA/0.01LUP/15Talc compared to those with 10% talc (Fig. 3f), suggesting a minor alteration in the polymer blend's crystalline lattice, induced by filler–matrix interactions. Comparable behavior was reported by Pal *et al.*,[56] when incorporating clay into a biodegradable polyhydroxybutyrate-*co*-hydroxyvalerate (PHBV)/PBAT blend.

The neat pCA formulations exhibited crystallinity values of 54.0% for pCTA and 55.8% for pCTEC (Table 4). The slightly higher crystallinity observed in pCTEC may stem from the hydroxyl (–OH) group in TEC, which enables additional hydrogen bonding between polymer chains and the plasticizer. According to Decroix *et al.*,[57] crystalline peaks in CA disappeared when the ethyl lactate plasticizer content exceeded ~19 wt%, highlighting structural modifications induced by plasticizers.

The addition of peroxide resulted in a reduction in crystallinity, decreasing from 54.0% to 53.6% for pCTA and from 55.8% to 48.6% for pCTEC, likely due to crosslinking points that interfere with the orderly arrangement of polymer chains during cooling from the melt. This correlates with improved complex viscosity observed after addition of LUP into pCTA or pCETC in rheological analysis (Fig. S1). As crosslinking, primarily initiated in the molten phase, increases, it limits the chain mobility necessary for forming well-organized crystalline domains.[44] These changes can affect mechanical performance where stronger chemical crosslinks restrict chain flexibility, shorten effective segment lengths, and cause uneven stress distribution under

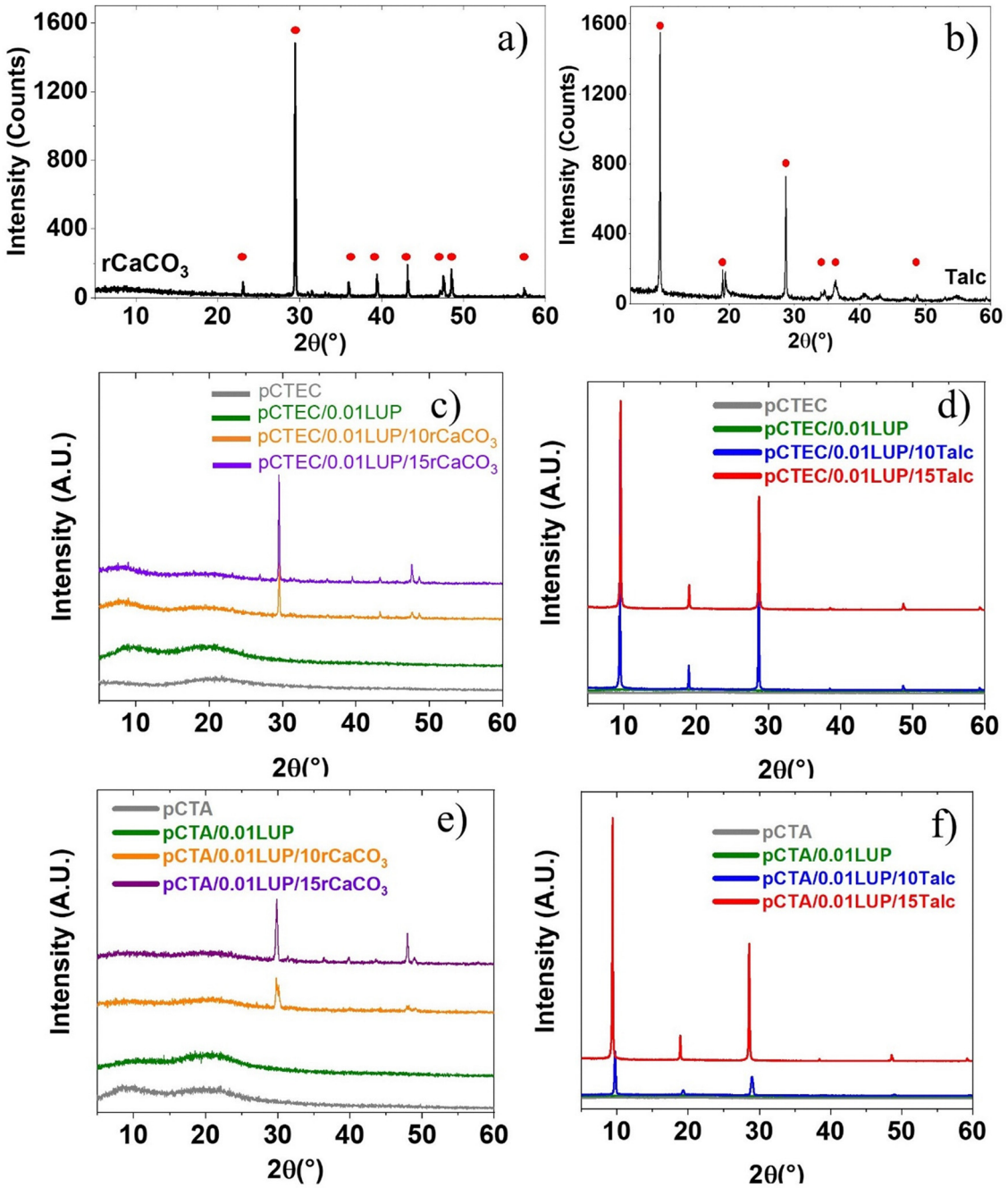

Fig. 3 XRD diffractograms of (a) $rCaCO_3$; (b) talc; (c) pCTEC/0.01LUP/10 or 15 $rCaCO_3$ composite and neat pCTEC films; (d) pCTEC/0.01LUP/10 or 15 talc composite and neat pCTEC films; (e) pCTA/0.01LUP/10 or 15 $rCaCO_3$ composite and neat pCTA films; (f) pCTA/0.01LUP/10 or 15 talc composite and neat pCTA films. While the addition of LUP reduced the crystallinity, fillers could improve crystalline organization in the pCTA or pCTEC matrix. pCTEC: plasticized cellulose acetate with triethyl citrate, pCTA: plasticized cellulose acetate with triacetin, TEC: triethyl citrate, TA: triacetin, LUP: luperox, and $rCaCO_3$: recycled calcium carbonate.

tensile loading, correlating with the reduced EB%[58] observed after LUP addition to pCA films (plasticized either with TA or TEC) (Section 3.1.1).

As previously discussed, mineral fillers such as $rCaCO_3$ or talc can influence the crystalline behavior of thermoplastic polymers due to their nucleating effect.[59] In this study, when 15 wt% $rCaCO_3$ was introduced, crystallinity increased markedly, reaching values close to 66–69% and almost 75–84% for talc (Table 4), confirming talc's superior nucleating ability. Similarly, Phetwarotai and Aht-Ong[60] found talc to be a more effective nucleating agent than $CaCO_3$ in PLA composites, though higher filler loadings may cause filler agglomeration and reduce the overall nucleation efficiency within the polymer matrix.

In conclusion, talc and $rCaCO_3$ resulted in more ordered crystalline structures in the pCTA or pCETC matrix, leading to

Table 4 Crystallinity degree calculated by X-ray diffraction for the neat pCA and its composites. pCTEC: plasticized cellulose acetate with triethyl citrate, pCTA: plasticized cellulose acetate with triacetin, TEC: triethyl citrate, TA: triacetin, LUP: luperox, $rCaCO_3$: recycled calcium carbonate

Sample	X_C (%)	Sample	X_C (%)
pCTA	54.0	pCTEC	55.8
pCTA/0.01LUP	53.6	pCTEC/0.01LUP	48.6
pCTA/0.01LUP/10Talc	73.7	pCTEC/0.01LUP/10Talc	71.6
pCTA/0.01LUP/15Talc	84.0	pCTEC/0.01LUP/15Talc	74.8
pCTA/0.01LUP/10$rCaCO_3$	57.7	pCTEC/0.01LUP/10$rCaCO_3$	63.7
pCTA/0.01LUP/15$rCaCO_3$	68.9	pCTEC/0.01LUP/15$rCaCO_3$	66.2

higher crystallinity and increased rigidity and stiffness, consistent with the mechanical results (Section 3.1.2).

3.3. Scanning electron microscopy (SEM)

SEM analysis was performed on $rCaCO_3$ and talc powder as well as a cross-section of the neat pCA and composite films to evaluate morphology, filler distribution, porosity, and structural defects.

As shown in Fig. S3 for talc and $rCaCO_3$ powder, the former is well known for its flat plate-like, shaped particles, with well-defined edges,[61] which makes talc an attractive reinforcement in polymeric composites. In contrast, $rCaCO_3$ consists of irregular, sharp-edged particles, in agreement with previous observations.[62]

Fig. 4 presents SEM photographs of pCTEC and pCTA films, along with their LUP-modified counterparts. Our earlier work[21] showed that pCTEC films have rougher surfaces than pCTA, though both display delaminated structures without pullouts due to the absence of fillers. As was explained in Section 3.1, LUP can introduce crosslinking, supported by rheological properties (Fig. S1 and S2) between polymer chains; excessive crosslinking may cause phase separation and cracking.[20] Even at the low peroxide loading used here (0.01 phr), LUP addition resulted in rougher surfaces with cracks compared to neat films. These defects correlate with reduced tensile performance, as crosslinks restrict chain mobility and act as defect sites,[44] explaining the sharp decrease in EB% for pCTEC/0.01LUP and pCTA/0.01LUP relative to neat films.

Fig. 5a–h exhibit the pCTA- and pCTEC-based composites containing 10 or 15 wt% talc or $rCaCO_3$. At first glance, the

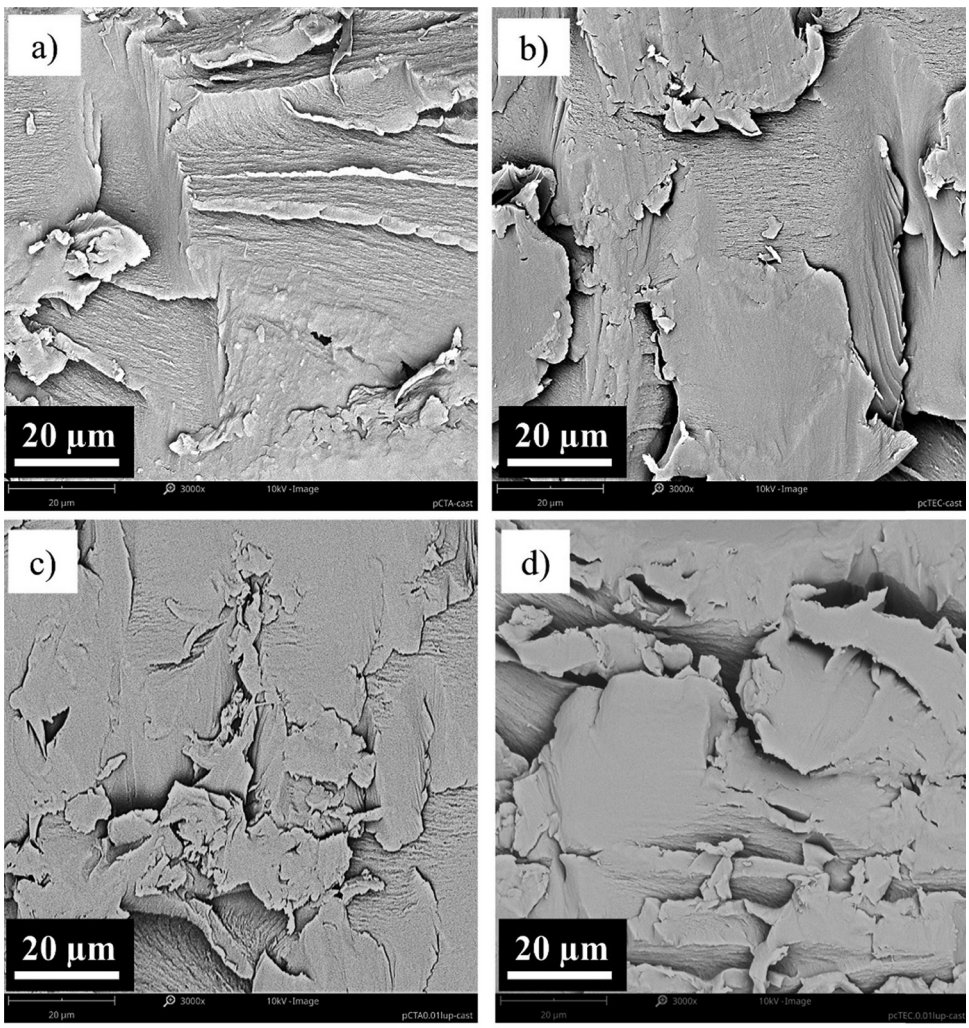

Fig. 4 The SEM images of cross-sections of films prepared in this study. (a) pCTA, (b) pCTEC, (c) pCTA/0.01LUP and (d) pCTEC/0.01LUP. [pCTEC: plasticized cellulose acetate with triethyl citrate, pCTA: plasticized cellulose acetate with triacetin, TEC: triethyl citrate, TA: triacetin, and LUP: luperox].

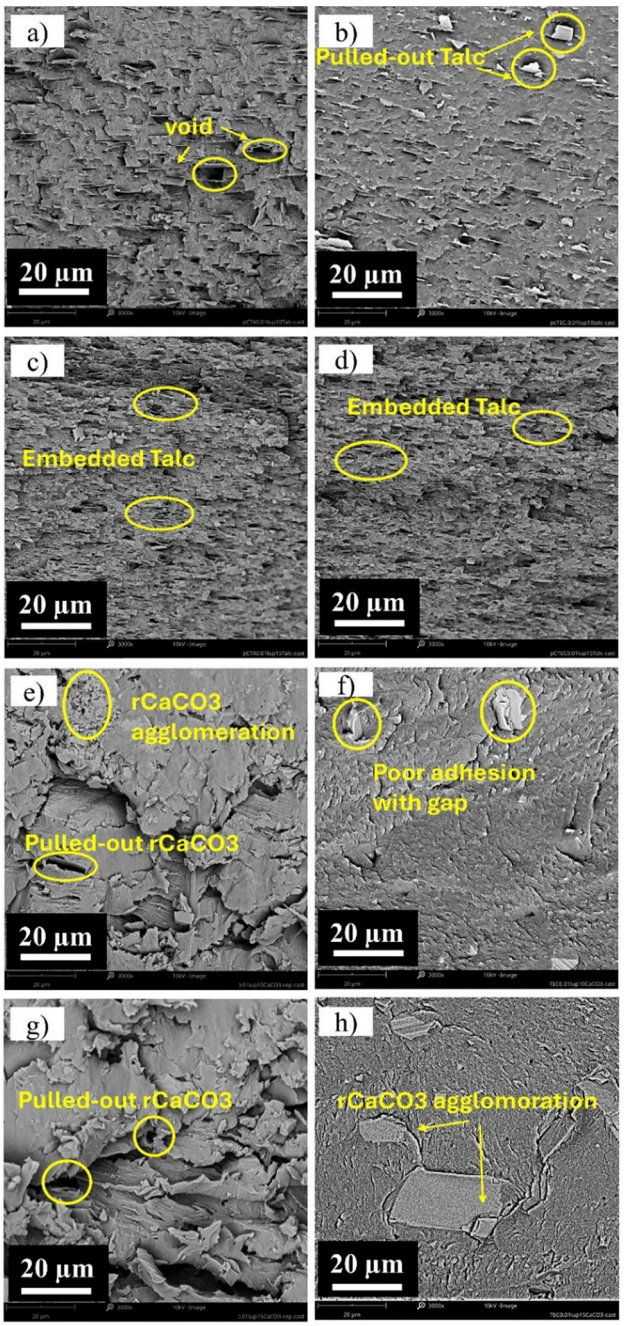

Fig. 5 The SEM images of cross-sections of composite films prepared in this study. (a) pCTA/0.01LUP/10Talc, (b) pCTEC/0.01LUP/10Talc, (c) pCTA/0.01LUP/15Talc and (d) pCTEC/0.01LUP/15Talc, (e) pCTA/0.01LUP/10r$CaCO_3$, (f) pCTEC/0.01LUP/10r$CaCO_3$, (g) pCTA/0.01LUP/15r$CaCO_3$, and (h) pCTEC/0.01LUP/15r$CaCO_3$. pCTEC: plasticized cellulose acetate with triethyl citrate, pCTA: plasticized cellulose acetate with triacetin, TEC: triethyl citrate, TA: triacetin, LUP: luperox, and r$CaCO_3$: recycled calcium carbonate.

talc-filled composites (Fig. 5a–d) showed a more homogenous dispersion of talc with better adhesion to the pCA matrix compared to the r$CaCO_3$-filled composites (Fig. 5e–h). This correlates with the significant improvements in mechanical properties (TS and EM) observed for pCTA/0.01LUP/10–15 wt% talc and pCTEC/0.01LUP/10–15 wt% talc relative to neat pCTA and pCTEC, respectively. The talc platelets' delamination and exfoliation in the presence of LUP promoted better interfacial adhesion, consistent with our previous findings.[21] Similar enhancements were reported when compatibilizers within LUP were incorporated into pCA/microcrystalline cellulose composites.[63] As shown in Fig. 5a–d, during cast film extrusion, the mobility of talc particles in the molten state enabled alignment of the platelets in the stretching direction, thereby strengthening interfacial adhesion. Comparable alignment was observed in the SEM of PP/talc composites prepared by injection molding,[59] as well as in poly(butylene succinate-*co*-butylene adipate) (PBSA)/talc[51] and PBAT/talc prepared by film blowing.[14] Although some talc pullouts and debonding voids were detected, especially in pCTEC/0.01LUP/10Talc and pCTA/0.01LUP/10Talc (Fig. 5a and b), most talc platelets were embedded within the polymer matrix. Increasing the talc loading to 15 wt% (Fig. 5c and d) further improved homogeneity and platelet embedding compared to 10 wt% composites. A similar effect of peroxide compatibilizers on PLA/talc composites has been reported.[61]

In contrast, r$CaCO_3$-filled composites (Fig. 5e–h) showed evident phase separation and filler agglomeration, more pronounced in TA-plasticized samples (Fig. 5e and g) than in those with TEC (Fig. 5f and h). This agrees with the mechanical results, where pCTEC/0.01LUP/10-15 wt% r$CaCO_3$ outperformed the TA-based composites in terms of TS, YM, and EB%. At 15 wt% loading (Fig. 5g and h), phase separation and agglomeration became more severe, regardless of the plasticizer type. Detachment of r$CaCO_3$ from the matrix (Fig. 5g and h) produced voids and gaps, especially in TA-plasticized composites, reflecting poor phase compatibility. Generally, higher filler content increases the likelihood of aggregation, leading to stress concentration zones and crack initiation sites that require less energy for crack propagation.[64] This explains the pronounced reduction in EB% of r$CaCO_3$-filled composites compared to neat pCA. Comparable aggregation was observed in PLA/$CaCO_3$ when the filler increased from 5 to 10 wt%.[65] The better adhesion observed for pCTEC-filled r$CaCO_3$ compared with pCTA-filled r$CaCO_3$, which directly resulted in higher EB%, can be attributed to the higher hydrophilicity of TEC than TA, where the –OH group in TEC promotes stronger interactions with r$CaCO_3$. A similar trend was reported for better $CaCO_3$ adhesion to poly-L-lactic acid (PLLA)-PEG-PLLA copolymers (more hydrophilic in the presence of PEG) compared to PLLA (hydrophobic).[62]

In summary, talc delamination and platelet alignment during film extrusion enhanced filler–matrix adhesion, leading to uniform dispersion. In contrast, r$CaCO_3$ composites exhibited agglomeration and poor compatibility, resulting in non-uniform dispersion and inferior mechanical performance.

3.4. Water contact angle and surface energy

The wettability test is used to assess the interaction between a liquid and a solid surface, with lower contact angles indicating stronger interactions and greater spreading.[66] Hydrophobic surfaces, typically composed of non-polar components, resist water

and exhibit moisture-repellent behavior. In contrast, hydrophilic surfaces readily attract water. Generally, a contact angle of less than 90° suggests a hydrophilic surface, while values exceeding 90° are indicative of hydrophobicity.[67] The surface wettability of the pCA and composite films was evaluated by measuring the contact angles of water and diiodomethane. A summary of the results is presented in Table 5, while corresponding images of the contact angle measurements for each formulation are available in the SI (Fig. S4 and S5).

Neat pCA samples exhibited contact angles of ~62° for water and ~33° for diiodomethane (Table 5) regardless of the plasticizer (TEC or TA), suggesting hydrophilic behavior. Shlush and Davidovich-Pinhas[33] reported that improved compatibility between a plasticizer and a polymer is typically associated with a lower contact angle. Based on solubility parameters, TEC would theoretically exhibit better compatibility with CA. However, this trend was not reflected in our results, as both plasticizers produced similar contact angle values, indicating that surface wettability was not significantly influenced by plasticizer type.

Incorporation of 0.01 phr LUP did not significantly alter contact angles, indicating minimal influence of low-level crosslinking on surface wettability (Table 5). The introduction of organic peroxide compounds can initiate two primary types of reactions: crosslinking and chain scissions.[19] While no directly comparable data were found in the open literature, a study by Kwon *et al.*[68] reported that crosslinking with glycidyl carbamate changed the WCA of glycidyl-carbamate-crosslinked polyurethane, and the trend in WCA does not necessarily match the trend in bulk crosslink density; this is attributed to differences in crosslinker flexibility and migration of hydrophobic segments to the surface during film formation.

Adding talc significantly increased WCAs, from ~62° for both neat pCTA and pCTEC samples to 69.4° and 74.0° for the pCTEC/0.01LUP/10Talc and pCTA/0.01LUP/10Talc, respectively (Table 5). Similarly, the diiodomethane contact angles increased from 32.3° (pCTA) and 34.1° (pCTEC) to 41.9° and 42.4° after addition of 10% Talc, reflecting the hydrophobic nature of the filler. Notably, no significant difference was observed between WCAs of the 10 wt% and 15 wt% talc-containing samples, in this study, with only a slight increase in diiodomethane contact angle at the higher filler loading. This aligns with previous studies reporting reduced hydrophilicity in polymer matrices upon incorporation of inorganic fillers.[40] A similar phenomenon was reported for PBAT-filled kaolin composites with varying loadings (1–5 wt%),[69] where the WCA increased from 70.5° to 93.1° upon incorporating 5 wt% kaolin into the PBAT matrix.

Like talc, $rCaCO_3$ reduces the hydrophilicity of the pCTA and the pCTEC matrix due to its inherently hydrophobic characteristics. The $rCaCO_3$ incorporation also increased contact angles, but to a lesser extent than talc. For example, the contact angles of water and diiodomethane increased by ~8% and ~21% in pCTA/0.01LUP/10$rCaCO_3$ compared to that in neat pCTA. The lower effectiveness compared to talc may be due to differences in particle morphology, as discussed in the SEM analysis (Section 3.3): talc has flat, platelet-like particles that align parallel to the flow direction during processing, while $rCaCO_3$ exhibits irregular, non-oriented shapes, affecting only the overall dispersion within the polymer matrix. Similarly, paper sheet-filled talc showed higher WCA than those with $CaCO_3$ due to talc's intrinsic hydrophobic nature.[70] Furthermore, increasing $rCaCO_3$ content from 10% to 15% did not significantly change the wettability, consistent with talc-filled composites.

Surface energy is a fundamental factor in understanding a material's wettability, as it quantifies the reversible energy required to generate a unit surface area under constant temperature and pressure.[71] Among the samples, pCTA and pCTEC exhibited the highest total surface energy, ~53 mN m^{-1}, using the harmonic and geometric mean methods (Table 5). This indicates pCA (plasticized with either TA or TEC) has the greatest affinity for wetting, consistent with its lower contact angle measurements.

In line with the contact angle trends, the incorporation of $rCaCO_3$ resulted in only a moderate reduction in surface energy, achieving a value of ~49 mN m^{-1} (Table 5). This suggests that $rCaCO_3$ was less effective than talc in enhancing hydrophobicity. Conversely, talc-containing composites exhibited the lowest

Table 5 Contact angle measurements and calculated total surface tension (γ), including its polar (γ^p) and dispersive (γ^d) components, for the neat pCTA and pCTEC samples and their composites. pCTEC: plasticized cellulose acetate with triethyl citrate, pCTA: plasticized cellulose acetate with triacetin, TEC: triethyl citrate, TA: triacetin, LUP: luperox, and $rCaCO_3$: recycled calcium carbonate

			Surface tension (mN m^{-1})					
	Contact angle (°)		Harmonic mean			Geometric mean		
Sample	Water	Diiodomethane	γ^p	γ^d	γ^{total}	γ^p	γ^d	γ^{total}
pCTA	62.3 ± 2.7	32.3 ± 2.0	15.9	43.5	59.4	10.0	43.3	53.3
pCTEC	61.6 ± 0.7	34.1 ± 1.7	16.4	42.8	59.2	10.7	42.4	53.1
pCTA/0.01LUP	62.5 ± 2.4	31.9 ± 2.2	15.8	43.7	59.5	9.9	43.4	53.3
pCTEC/0.01LUP	60.3 ± 0.6	44.0 ± 0.6	18.0	38.3	56.3	13.1	37.5	50.6
pCTA/0.01LUP/10 Talc	74.0 ± 2.1	41.9 ± 0.8	11.2	39.3	50.5	5.9	38.7	44.6
pCTA/0.01LUP/15 Talc	73.6 ± 1.5	44.8 ± 1.0	11.7	37.9	49.6	6.5	37.1	43.6
pCTEC/0.01LUP/10 Talc	69.4 ± 0.5	42.4 ± 1.1	13.4	39.1	52.5	8.1	38.4	46.5
pCTEC/0.01LUP/15 Talc	70.6 ± 0.5	43.1 ± 2.9	12.9	38.7	51.6	7.6	38.0	45.6
pCTA/0.01LUP/10 $rCaCO_3$	67.2 ± 0.5	39.1 ± 1.7	14.1	40.6	54.7	8.6	40.1	48.7
pCTA/0.01LUP/15 $rCaCO_3$	65.9 ± 1.1	43.6 ± 3.9	15.2	38.5	53.7	10.0	37.8	47.8
pCTEC/0.01LUP/10 $rCaCO_3$	67.7 ± 0.2	37.3 ± 1.2	13.8	41.4	55.2	8.1	40.9	49.0
pCTEC/0.01LUP/15 $rCaCO_3$	64.0 ± 1.2	41.2 ± 0.8	15.9	39.6	55.5	10.5	39.0	49.5

surface energy, with the pCTA/0.01LUP/15Talc formulation reaching 43.6 mN m^{-1} (Table 5), corresponding to the highest measured contact angles for both water and diiodomethane. This reduction in surface energy and enhanced hydrophobicity is likely due to the orientation of the talc platelets and polymer chains during processing, which promotes higher crystallinity as supported by XRD analysis (Section 3.2). Supporting these findings, Olewnik and Richert[72] found that adding 5 wt% montmorillonite led to a slight decrease in contact angle, by about 1.5%, highlighting how the amount of filler can influence the surface energy and wettability.

3.5. Water vapor permeability (WVP) and oxygen permeability (OP)

For packaging applications, films must provide high water vapor and oxygen barriers to prevent moisture and oxygen permeation, thereby reducing microbial growth, spoilage, and quality loss. Barrier performance depends on penetrant characteristics (shape, size, and hydrophobicity), filler properties, polymer chain orientation, and processing method.[73] The OP and WVP of neat pCTA, pCTEC, and their composite films are shown in Fig. 6 and Table S2 (SI).

3.5.1. Oxygen permeability. Neat pCTEC exhibited a higher OP (2462.99 cc mil/m^2 day) than pCTA (1986.93 cc mil/m^2 day). Several factors contribute to this difference: (I) more efficient plasticization effect of TEC, which disrupts polymer chain packing and increases free volume, and OP. (II) Film stretching during the casting process may further align TA, promoting tighter packing and lower OP compared with the bulkier TEC.

Adding LUP alone had little effect on barrier performance. pCTA/0.01LUP showed ~32% higher OP, while pCTEC/0.01LUP remained unchanged compared to the neat films, consistent with minimal WCA changes for pCTA and a slight decrease for pCTEC. In contrast, incorporating talc within LUP significantly enhanced the oxygen barrier properties. The best performance was observed in pCTA/0.01LUP/15Talc (34% improvement) and pCTEC/0.01LUP/15Talc (38% improvement) *versus* neat pCTA and pCTEC films, respectively. The relative improvements in water vapor barrier properties of pCA-based composite films, compared with neat pCA, are as follows:

pCTA-based composite films:

pCTA/0.01LUP/15Talc (34.37%) > pCTA/0.01LUP/10Talc (21.19%) > pCTA/0.01LUP/10r$CaCO_3$ (13.60%) > pCTA/0.01LUP/15r$CaCO_3$ (11.02%)

pCTEC-based composite films:

pCTEC/0.01LUP/15Talc (38.27%) > pCTEC/0.01LUP/10Talc (26.19%) > pCTEC/0.01LUP/15r$CaCO_3$ (2.48%) > pCTEC/0.01LUP/10r$CaCO_3$ (1.85%)

These results demonstrate that talc-filled composites outperformed r$CaCO_3$-filled systems, which correlated with SEM images showing deep talc embedding in the pCA matrix, compared with agglomeration of r$CaCO_3$ in r$CaCO_3$-filled pCA (plasticized either with TA or TEC). OP depends on the diffusion rate of oxygen over the amorphous region of the polymer matrix.[73] This correlates with the highest %crystallinity improvement of pCTA/0.01LUP/15Talc (by 55%) and pCTEC/0.01LUP/15Talc (by 34%) compared with the neat pCTA or pCTEC, respectively. Talc's platelet structure facilitates delamination, exfoliation, and alignment during film stretching, forming a talc-embedded pCA (plasticized either with TA or TEC) layer against OP, which results in a tortuous diffusion path, thereby reducing OP, similar to effects reported for the talc-filled PLA films.[75]

On the other hand, pCTA-filled r$CaCO_3$ and pCTEC-filled r$CaCO_3$, only slightly reduced the OP compared with neat pCTA and pCTEC, respectively, which can be due to reduction of the overall amorphous structure of pCA and imparted crystallinity after the addition of crystalline r$CaCO_3$ particles. This is consistent with the improved %crystallinity after addition of 10 or 15 wt% r$CaCO_3$ into pCTA/0.01LUP or pCTEC/0.01LUP. Similar observations were reported in the case of calcium carbonate–cellulose composite films[76] and PP-filled pretreated $CaCO_3$ composite films.[77]

3.5.2. Water vapor permeability. Comparing neat pCTA and pCTEC, the latter showed ~2× higher WVP due to the greater hydrophilicity of TEC *versus* TA, which enhances

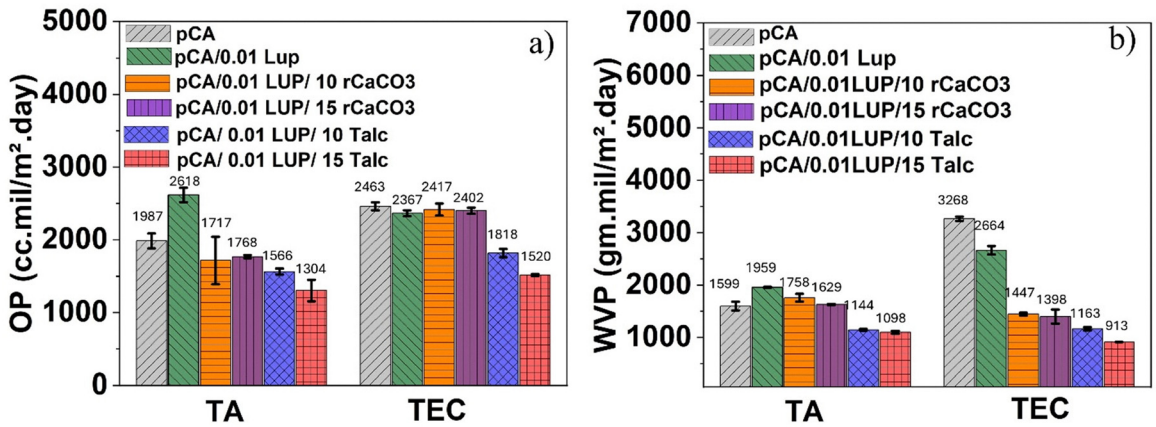

Fig. 6 (a) Oxygen permeability, and (b) water vapor permeability of neat pCTA and pCTEC films and their composite films. pCTA showed higher barriers against oxygen and water vapor permeation in comparison with pCTEC. The pCA-filled talc composite films exhibited superior barriers to both water vapor and oxygen compared with pCA-filled r$CaCO_3$. pCTEC: plasticized cellulose acetate with triethyl citrate, pCTA: plasticized cellulose acetate with triacetin, TEC: triethyl citrate, TA: triacetin, LUP: luperox, and r$CaCO_3$: recycled calcium carbonate.

interactions with water vapor. Studies showed that TEC has higher water solubility (hydrophilicity) than TA (*i.e.*, 65 g liter^{-1} *vs.* 58 g liter^{-1}, respectively).[74] Teixeira *et al.*[78] similarly reported higher WVP in pCA plasticized with glycerol than with TEC, attributed to glycerol's stronger hygroscopicity. Higher WVP of pCTEC than pCTA is also consistent with pCTEC's higher WVA_{eq} calculated in Table S1 (SI).

Similar to the OP trends, adding LUP alone to pCTA did not improve barrier performance: pCTA/0.01LUP exhibited ~22% higher WVP compared to the neat film, consistent with its reduced crystallinity. In contrast, pCTEC/0.01LUP showed an ~18% reduction in WVP, though its crystallinity decreased compared to neat pCTEC. As mentioned earlier, several factors contribute to barrier performance which can compensate for the inferior crystallinity of pCTEC/0.01LUP over neat pCTEC.

The incorporation of LUP with 10 or 15 wt% $rCaCO_3$ or talc to pCTA or pCTEC showed the same trend in reduction of WVP, while talc more effectively reduced it, compared with their pCA/0.01LUP films. The best water vapor barrier was achieved from pCTA/0.01LUP/15Talc (increased by ~31%) and pCTEC/0.01LUP/15Talc (increased by ~72%) *versus* pCTA and pCTEC, respectively.

The WVP is mainly governed by the solubility of penetrants in the polymer, which depends on polymer–permeant interactions.[79] Talc, with its hydrophobic, plate-like morphology,[80] repels moisture and enhances barrier properties in pCTA- or pCTEC-filled talc composites. This effect aligns with the talc-filled composites' higher WCA (greater hydrophobicity) and %crystallinity compared to $rCaCO_3$-filled systems. Increased hydrophobicity reduces the solubility coefficient, thereby improving water vapor resistance.[73] Additionally, parallel alignment of talc plates during film casting creates tortuous diffusion paths that lengthen permeation routes, reducing WVP. The same behavior of talc particles has been reported in previous literature reports.[14,51] Similarly, addition of talc into PLA composites increased the barrier against water vapor by more than 50% compared with neat PLA.[81]

On the other hand $rCaCO_3$ particles are more hydrophilic than talc,[82] which makes them more favorable for water interactions and moisture absorption (as discussed in the FTIR results provided in Fig. S6), thereby increasing the WVP. The $rCaCO_3$ spherical shape can lead to poor interfacial adhesion and aggregation in the pCA (TA- or TEC-plasticized) matrix, as observed in the SEM photographs of the pCTEC-filled or pCTA-filled $rCaCO_3$. Such aggregation disrupts the matrix integrity and forms microvoids that facilitate water vapor transport. Similarly, Surya *et al.*[83] reported higher WVP in $CaCO_3$-filled biocomposites due to filler agglomeration and pull-out, which created gaps that enhanced moisture penetration.

The relative improvements in water vapor barrier properties of the pCA-based composite films, compared with neat pCA, are as follows:

pCTA-based composite films:

pCTA/0.01LUP/15Talc (31.29%) > pCTA/0.01LUP/10Talc (28.42%) > pCTA/0.01LUP/15r$CaCO_3$ (−1.88%) > pCTA/0.01LUP/10r$CaCO_3$ (−9.97%)

pCTEC-based composite films:

pCTEC/0.01LUP/15Talc (72%) > pCTEC/0.01LUP/10Talc (64%) > pCTEC/0.01LUP/15r$CaCO_3$ (57%) > pCTEC/0.01LUP/10r$CaCO_3$ (55%)

In conclusion, pCTA showed higher barriers against WVP and OP in comparison with pCTEC. The pCTEC- or pCTA-filled talc composites developed in this study exhibited superior barriers to both oxygen and water vapor *versus* pCTA- or pCETC-filled $rCaCO_3$, highlighting their potential as an eco-friendly alternative for traditional packaging materials.

3.6. Thermogravimetric analysis (TGA)

The thermal stability of neat pCTA and pCTEC and composite films was evaluated by TGA, with results shown in Fig. 7 and Table 6, and the corresponding DTG curves are shown in Fig. S7. All samples exhibited two-step degradation: plasticizer loss (226–323 °C) and CA decomposition (376–384 °C).

The pCTEC displayed markedly higher stability than pCTA in terms of their T_{onset}, 211.51 °C compared to 143.35 °C, respectively. This difference can arise from TEC's free –OH group, which enables additional hydrogen bonding with CA, whereas TA lacks such groups, which results in a lower number of hydrogen bonding. This is further reflected in the T_{max} of plasticizers, where T_{maxTEC} (315.37 °C) greatly surpassed T_{maxTA} (226.25 °C), a trend also maintained after adding LUP and fillers (Table 6).

LUP incorporation improved stability in pCTA, increasing the T_{onset} by ~28 °C due to crosslinking, consistent with its higher complex viscosity and reduced elongation at break. Similarly, the addition of LUP to the blend of pCA/PBAT[19] resulted in an increase in the T_{onset} due to the crosslinking effect induced by organic peroxide. In contrast, pCTEC/0.01LUP showed a slight decrease in T_{onset} compared with pCTEC.

Adding 10–15 wt% talc to pCTA/0.01LUP significantly increased the T_{onset} (by ~43 °C and ~23 °C, respectively). Talc hydroxyl groups ($Mg_3Si_4O_{10}(OH)_2$) can form hydrogen bonds with pCTA and interact with free radicals generated by LUP, enhancing stability. Similarly, Hong *et al.*[64] reported the reaction between –OH groups in talc with PLA and epoxidized soybean oil. For pCTEC/0.01LUP after the addition of 10 or 15 wt% talc, the T_{onset} increased which was more pronounced in pCTEC/0.01LUP/15Talc for which T_{onset} increased by ~15 °C, compared with pCTEC/0.01LUP. Similarly, addition of talc as well as increasing the talc content in the blend of PP/thermoplastic polyurethane resulted in significant improvements in $T_{5\%}$ and T_{max}.[84]

The addition of 10 or 15 wt% $rCaCO_3$ into pCTA/0.01LUP likewise enhanced the thermal stability as their T_{onset} increased. pCTA/0.01LUP/10r$CaCO_3$ and pCTA/0.01LUP/15r$CaCO_3$ showed ~14 °C and ~12 °C higher T_{onset}, respectively, than pCTA/0.01LUP. Similarly, pCTEC/0.01LUP/10r$CaCO_3$ and pCTEC/0.01LUP/15r$CaCO_3$ showed ~13 °C and ~7 °C higher T_{onset}, respectively, than pCTEC/0.01LUP. This improvement likely results from filler–matrix interactions and hydrogen bonding, consistent with reports of $CaCO_3$ increasing the $T_{5\%}$ in PLLA-based block copolymers.[62]

Notably, the T_{maxCA} of composites remained essentially unchanged after adding LUP, talc, or $rCaCO_3$, highlighting the

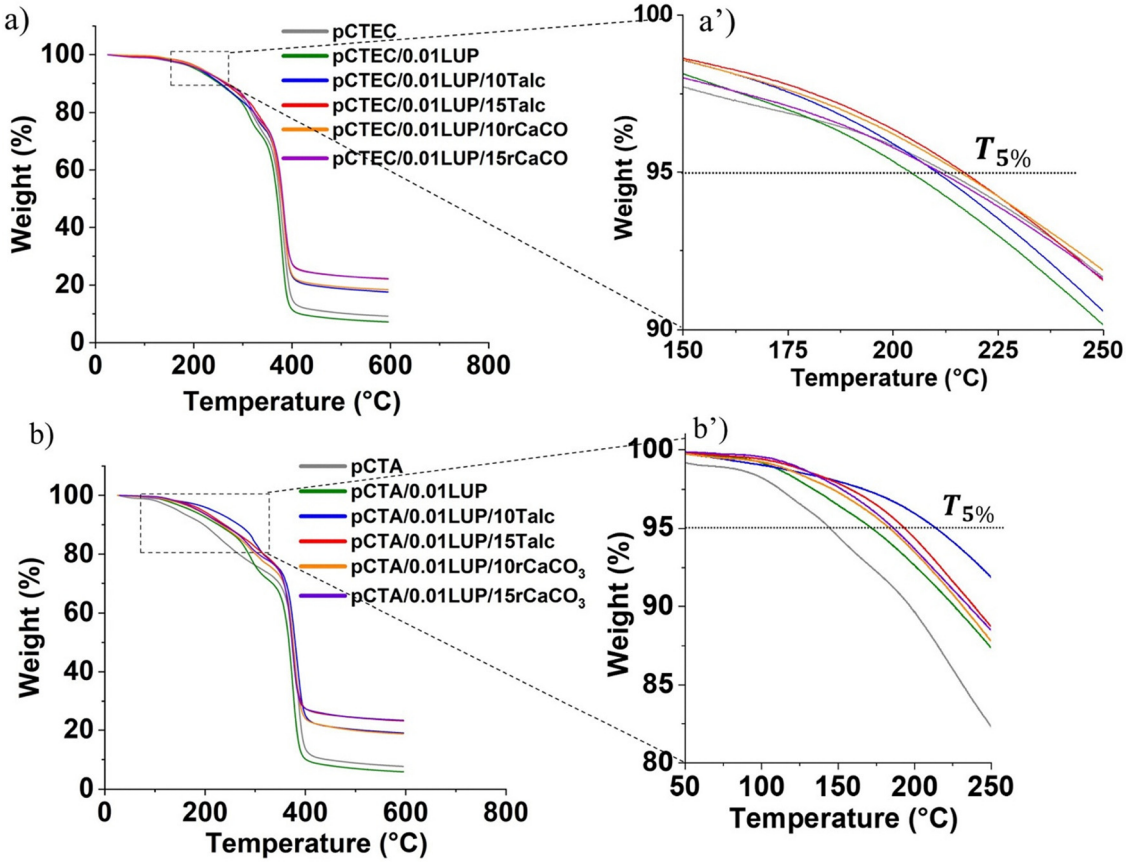

Fig. 7 Thermograms of neat pCTA and pCTEC films and composite films. (a) and (a′) pCTEC-based formulations. (b) and (b′) pCTA-based formulations. pCTEC: plasticized cellulose acetate with triethyl citrate, pCTA: plasticized cellulose acetate with triacetin, TEC: triethyl citrate, TA: triacetin, LUP: luperox, and $rCaCO_3$: recycled calcium carbonate.

Table 6 Data from thermogravimetric analysis of neat pCTA and pCTEC films and composite films. pCTEC: plasticized cellulose acetate with triethyl citrate, pCTA: plasticized cellulose acetate with triacetin, TEC: triethyl citrate, TA: triacetin, LUP: luperox, and $rCaCO_3$: recycled calcium carbonate

Formulation	$T_{onset\,(5\%)}$	T_{maxTA}	T_{maxTEC}	T_{maxCA}	Residue (%)
pCTA	143.35 (2.04)	226.25 (3.79)	—	383.00 (1.90)	8.06 (0.38)
pCTEC	211.51 (1.72)	—	315.37 (0.71)	383.78 (0.43)	8.85 (0.56)
pCTA/0.01LUP	171.16 (1.30)	293.92 (2.00)	—	379.99 (6.54)	6.74 (1.05)
pCTEC/0.01LUP	202.00 (2.91)	—	315.37 (3.89)	381.65 (4.24)	8.22 (1.35)
pCTA/0.01LUP/10Talc	213.78 (0.14)	294.22 (2.42)	—	380.46 (4.48)	19.50 (0.69)
pCTEC/0.01LUP/10Talc	207.52 (3.93)	—	323.70 (3.23)	382.03 (2.07)	16.45 (1.71)
pCTA/0.01LUP/15Talc	193.80 (0.36)	274.25 (3.86)	—	377.21 (3.13)	23.20 (0.10)
pCTEC/0.01LUP/15Talc	216.82 (0.03)	—	322.89 (0.85)	380.57 (2.58)	22.67 (0.70)
pCTA/0.01LUP/10$rCaCO_3$	185.37 (2.52)	298.80 (1.56)	—	376.57 (2.07)	18.77 (0.05)
pCTEC/0.01LUP/10$rCaCO_3$	215.07 (1.22)	—	310.06 (5.93)	379.32 (4.87)	18.82 (0.62)
pCTA/0.01LUP/15$rCaCO_3$	182.92 (4.66)	290.21 (2.12)	—	377.24 (4.94)	23.36 (0.09)
pCTEC/0.01LUP/15$rCaCO_3$	209.37 (2.58)	—	312.30 (1.99)	380.05 (5.24)	23.45 (1.42)

intrinsic stability of CA. This observation agrees with prior studies where fillers and compatibilizers did not affect CA decomposition.[41]

The remaining mass after the material has been heated to 600 °C, represents the amount of non-volatile components. The neat pCTEC and pCTA showed almost similar residue% which was 8.06 and 8.85%, respectively, attributed to any non-volatile content in the CA. Similarly, Lee *et al.*[85] reported 11.9% residual mass for CA. Residues of composites aligned approximately with expected filler loadings, with minor deviations attributed to intercomponent reactions or variations in sample preparation.

Overall, pCTEC showed much higher thermal stability than pCTA in terms of T_{onset} and T_{maxTEC}, which was consistent across almost all pCTEC-based composites as well.

Conclusions

This work establishes hot-melt extrusion as a practical and industry-relevant route for producing sustainable plasticized cellulose acetate (pCA) composite films, offering a scalable

alternative to solvent-based processing. The study highlights how the careful integration of bio-based or petrochemical plasticizers with mineral fillers can be strategically used to tune the balance between stiffness, toughness, thermal resistance, and interfacial behavior in pCA systems.

More importantly, the results reveal the critical role of filler morphology and filler–matrix interactions, in the presence of a small amount of peroxide, in influencing end-use performance. Talc's inherent platelet structure and its ability to align during extrusion produced stronger interfacial adhesion, more effective stress transfer, improved barrier properties, and more uniform morphologies compared with recycled $CaCO_3$. These insights underscore how filler selection and their interactions with plasticized CA can be leveraged to engineer composites with targeted mechanical, thermal, and surface properties.

Overall, the study provides a framework for designing next-generation biodegradable pCA composite films with enhanced functionality. By demonstrating that low-acetyl CA plasticized with TEC reinforced with talc can achieve the mechanical and barrier characteristics relevant for flexible packaging, this work contributes to the broader transition away from petroleum-based materials toward more circular, environmentally responsible solutions.

Author contributions

Fatemeh Jahangiri: methodology; investigation; formal analysis; data curation; writing – original draft. Matias Menossi: methodology; investigation; formal analysis; data curation; writing – original draft. Manjusri Misra: conceptualization; investigation; validation; resources; writing – review and editing; funding acquisition; project administration; supervision. Amar K. Mohanty: conceptualization; investigation; validation; resources; writing – review and editing; funding acquisition; project administration; supervision.

Conflicts of interest

The authors declare that they have no conflicts of interest.

Data availability

Data for this article, including raw data and the origin files for the figures and tables are available at Borealis https://doi.org/10.5683/SP3/OQTIXX.

Supplementary information (SI): calculation of DS and MW of the cellulose acetate, rheological properties (Fig. S1 and S2), SEM images of $rCaCO_3$ and talc powder (Fig. S3), water contact angle images (Fig. S4 and S5), WVA_{eq} values (Table S1), WVP and OP values (Table S2), FTIR analysis (Fig. S6), and DTG graphs (Fig. S7). See DOI: https://doi.org/10.1039/d5ma01323b.

Acknowledgements

The authors are grateful for the financial support from (i) the Ontario Agri-Food Innovation Alliance-Bioeconomy for Industrial Uses Research Program (Project No. 030648, 030671 and 030699) and the Ontario Agri-Food Research Initiative (Project No. 056442); (ii) the Ontario Ministry of Colleges and Universities (MCU), Ontario, Canada Research Fund – Research Excellency ORF-RE11 (Project No. 056106); (iii) the Natural Sciences and Engineering Research Council of Canada (NSERC), the Canada Research Chairs (CRC) program Project No. 460788; and (iv) the NSERC Alliance Grants Program (Project No. 401769) along with the partner industry Competitive Green Technologies, Lamington, Ontario, Canada (Project No. 055427) to carry out this research.

References

1 A. K. Mohanty, F. Wu, R. Mincheva, M. Hakkarainen, J. M. Raquez, D. F. Mielewski, R. Narayan, A. N. Netravali and M. Misra, *Nat. Rev. Methods Primers*, 2022, **2**, 46.
2 S. Sid, R. S. Mor, A. Kishore and V. S. Sharanagat, *Trends Food Sci. Technol.*, 2021, **115**, 87–104.
3 M. Menossi, M. Misra and A. K. Mohanty, *Prog. Polym. Sci.*, 2024, **160**, 101919.
4 A. C. Wibowo, M. Misra, H.-M. Park, L. T. Drzal, R. Schalek and A. K. Mohanty, *Composites, Part A*, 2006, **37**, 1428–1433.
5 K. Meereboer, A. Pal, M. Misra and A. Mohanty, *ACS Omega*, 2020, **5**(24), 14221–14231.
6 N. Yadav and M. Hakkarainen, *Chemosphere*, 2021, **265**, 128731.
7 A. Raza, S. Farrukh, A. Hussain, I. Khan, M. H. D. Othman and M. Ahsan, *Membranes*, 2021, **11**, 245.
8 H.-M. Park, M. Misra, L. T. Drzal and A. K. Mohanty, *Biomacromolecules*, 2004, **5**, 2281–2288.
9 A. Bonifacio, L. Bonetti, E. Piantanida and L. De Nardo, *Eur. Polym. J.*, 2023, **197**, 112360.
10 X. Dreux, J.-C. Majesté, C. Carrot, A. Argoud and C. Vergelati, *Carbohydr. Polym.*, 2019, **222**, 114973.
11 E. Pesaranhajiabbas, A. K. Mohanty, M. S. Al-Abdul-Wahid and M. Misra, *SPE Polym.*, 2024, **5**, 217–227.
12 A. Charvet, C. Vergelati and D. R. Long, *Carbohydr. Polym.*, 2019, **204**, 182–189.
13 C. Y. Bao, D. R. Long and C. Vergelati, *Carbohydr. Polym.*, 2015, **116**, 95–102.
14 B. E. Itabana, A. K. Pal, A. K. Mohanty and M. Misra, *Food Packag. Shelf Life*, 2023, **39**, 101147.
15 U. L. Muhammad, M. Y. Musa, Y. Usman and A. B. Nasir, *Am. J. Phys. Chem.*, 2018, **7**, 23–28.
16 J. Lu, Z. Lu, X. Li, H. Xu and X. Li, *J. Cleaner Prod.*, 2015, **92**, 223–229.
17 T. Zhang, Á. G. Rivas, X. F. Fernandez, N. Li, E. Gucho, L. Zhu, A. Bijl, J. L. Llacuna and S. He, *Renewable Energy*, 2024, **236**, 121429.
18 A. K. Mohanty, S. Vivekanandhan, J.-M. Pin and M. Misra, *Science*, 2018, **362**, 536–542.
19 M. Menossi, M. Misra and A. K. Mohanty, *ACS Appl. Polym. Mater.*, 2024, **6**, 10202–10217.
20 F. Wu, M. Misra and A. K. Mohanty, *RSC Adv.*, 2019, **9**, 2836–2847.
21 F. Jahangiri, M. Menossi, M. Misra and A. K. Mohanty, *J. Appl. Polym. Sci.*, 2025, e57973.

22 A. John, Y. Chen and J. Kim, *Composites, Part B*, 2012, **43**, 522–525.
23 Y. Leong, Z. M. Ishak and A. Ariffin, *J. Appl. Polym. Sci.*, 2004, **91**, 3327–3336.
24 S. Akter, Y. Akter, S. Islam, S. Dewanjee, S. Ahmed and M. S. Alam, *Ind. Chem.*, 2019, **5**(1), 1000131.
25 B. S. Tuen, A. Hassan and A. Abu Bakar, *J. Vinyl Addit. Technol.*, 2012, **18**, 76–86.
26 C. S. Marques, R. R. A. Silva, T. R. Arruda, A. L. V. Ferreira, T. V. D. Oliveira, A. R. F. Moraes, M. V. Dias, M. C. D. Vanetti and N. D. F. F. Soares, *Polysaccharides*, 2022, **3**, 277–291.
27 A. W. Cindradewi, R. Bandi, C.-W. Park, J.-S. Park, E.-A. Lee, J.-K. Kim, G.-J. Kwon, S.-Y. Han and S.-H. Lee, *Polymers*, 2021, **13**, 2990.
28 N. Špánić, V. Jambreković, M. Šernek and S. Medved, *Int. J. Polym. Sci.*, 2019, 1065024.
29 F. J. Rodríguez, M. J. Galotto, A. Guarda and J. E. Bruna, *J. Food Eng.*, 2012, **110**, 262–268.
30 E. Shlush and M. Davidovich-Pinhas, *Carbohydr. Polym. Technol. Appl.*, 2025, **10**, 100746.
31 R. Kabiri and H. Namazi, *Cellulose*, 2014, **21**, 3527–3539.
32 H. Abd El-Rehim, H. Kamal, E.-S. A. Hegazy, E. S. Soliman and A. Sayed, *Radiat. Phys. Chem.*, 2018, **153**, 180–187.
33 E. Shlush and M. Davidovich-Pinhas, *Food Packag. Shelf Life*, 2023, **40**, 101206.
34 M. Oliviero, E. Lamberti, L. Cafiero, B. Pace, M. Cefola, G. Gorrasi, A. Sambandam and A. Sorrentino, *Mater. Chem. Phys.*, 2023, **310**, 128469.
35 D. Bondeson, P. Syre and K. O. Niska, *J. Biobased Mater. Bioenergy*, 2007, **1**, 367–371.
36 R. Quintero, M. Galotto, F. Rodriguez and A. Guarda, *Packag. Technol. Sci.*, 2014, **27**, 495–507.
37 C. Herniou, J. R. Mendieta and T. J. Gutiérrez, *Food Hydrocolloids*, 2019, **89**, 67–79.
38 M. Menossi, F. Salcedo, J. Capiel, M. Adler, V. A. Alvarez and L. N. Ludueña, *J. Polym. Res.*, 2022, **29**, 285.
39 M. Menossi, F. Salcedo, A. Y. Mansilla, V. A. Alvarez and L. N. Ludueña, *J. Appl. Polym. Sci.*, 2025, **142**, e56933.
40 M. Menossi, M. Misra and A. K. Mohanty, *Macromol. Mater. Eng.*, 2025, 2400434.
41 L. D. Hernandez-Ruiz, M. Hassan, T. Wang, A. K. Mohanty and M. Misra, *Compos., Part C: Open Access*, 2025, 100606.
42 F. Wu, M. Misra and A. K. Mohanty, *Polym. Degrad. Stab.*, 2020, **173**, 109066.
43 C. González-Sánchez, A. Martínez-Aguirre, B. Pérez-García, J. Acosta, C. Fonseca-Valero, M. De La Orden, C. Sánchez and J. M. Urreaga, *Composites, Part A*, 2016, **80**, 285–291.
44 S.-Q. Liu, W.-G. Gong and B.-C. Zheng, *J. Macromol. Sci., Part B:Phys.*, 2014, **53**, 67–77.
45 J. Zhu, C. Abeykoon and N. Karim, *Int. J. Lightweight Mater. Manuf.*, 2021, **4**, 370–382.
46 M. Boruvka, P. Lenfeld, P. Brdlik and L. Behalek, *IOP Conf. Ser.:Mater. Sci. Eng.*, 2015, **87**, 012085.
47 L. Botta, R. Teresi, V. Titone, G. Salvaggio, F. P. La Mantia and F. Lopresti, *Polymers*, 2021, **13**, 3953.
48 D. Phothisarattana, P. Wongphan, K. Promhuad, J. Promsorn and N. Harnkarnsujarit, *Polymers*, 2021, **13**, 4192.
49 S. A. Oleyaei, Y. Zahedi, B. Ghanbarzadeh and A. A. Moayedi, *Int. J. Biol. Macromol.*, 2016, **89**, 256–264.
50 N. A. Musa, N. Mohamad, H. E. Ab Maulod, J. Abd Razak, M. E. Abd Manaf, M. I. Shueb, P. R. Zakyron and M. M. A. Abdullah, *Malay. J. Micros.*, 2025, **21**, 112–122.
51 D. Nath, A. K. Pal, M. Misra and A. K. Mohanty, *Macromol. Mater. Eng.*, 2023, **308**, 2300214.
52 Z. Hu, S. Zheng, M. Jia, X. Dong and Z. Sun, *Adv. Powder Technol.*, 2017, **28**, 1372–1381.
53 N. Sulimai, R. A. Rani, Z. Khusaimi, S. Abdullah, M. Salifairus, S. Alrokayan, H. Khan, P. Sermon and M. Rusop, *Mater. Sci. Eng., B*, 2019, **243**, 78–85.
54 R. R. De Freitas, A. M. Senna and V. R. Botaro, *Ind. Crops Prod.*, 2017, **109**, 452–458.
55 L. Jing, Y. Wang, J. Li, X. Lin, L. Liu, Y. Chen, H. Liu and Z. Ying, *Int. J. Biol. Macromol.*, 2024, **269**, 131894.
56 A. K. Pal, F. Wu, M. Misra and A. K. Mohanty, *Composites, Part B*, 2020, **198**, 108141.
57 C. Decroix, Y. Chalamet, G. Sudre and V. Caroll, *Carbohydr. Polym.*, 2020, **237**, 116072.
58 J. Huang, P. Fu, W. Li, L. Xiao, J. Chen and X. Nie, *RSC Adv.*, 2022, **12**(36), 23048–23056.
59 L. A. Castillo, S. E. Barbosa and N. J. Capiati, *J. Polym. Res.*, 2013, **20**, 1–9.
60 W. Phetwarotai and D. Aht-Ong, *J. Therm. Anal. Calorim.*, 2017, **127**, 2367–2381.
61 S. B. Park, Y. J. Lee, K. H. Ku and B. J. Kim, *J. Appl. Polym. Sci.*, 2022, **139**, 51488.
62 P. Srihanam, W. Thongsomboon and Y. Baimark, *Polymers*, 2023, **15**, 301.
63 I. García-Castellanos, D. Nath, R. Krishnan, M. Misra and A. K. Mohanty, *ACS Sustain. Res. Manage.*, 2025, **2**(4), 594–604.
64 Y. Hong, L. Chen, G. Song, D. Bassir, S. Cheng, X. Shi, H. Liu and G. Tang, *Polym. Compos.*, 2018, **39**, E1618–E1625.
65 K. Piekarska, E. Piorkowska and J. Bojda, *Polym. Test.*, 2017, **62**, 203–209.
66 F. Jahangiri, A. K. Mohanty, A. K. Pal, S. Shankar, A. Rodriguez-Uribe, R. Clemmer, S. Gregori and M. Misra, *Prog. Org. Coat.*, 2024, **189**, 108270.
67 D. Ahmad, I. Van Den Boogaert, J. Miller, R. Presswell and H. Jouhara, *Energy Sources, Part A*, 2018, **40**, 2686–2725.
68 Y. R. Kwon, J. H. Park, H. C. Kim, S. K. Moon and D. H. Kim, *Polymers*, 2024, **16**, 2794.
69 R. Venkatesan, K. Alagumalai and S.-C. Kim, *Polymers*, 2023, **15**, 1710.
70 V. S. Chauhan and N. K. Bhardwaj, *Appita*, 2013, **66**, 66–72.
71 A. Goswami, S. C. Pillai and G. McGranaghan, *Surf. Interfaces*, 2021, **25**, 101143.
72 E. Olewnik and J. Richert, *Polym. Compos.*, 2015, **36**, 17–25.
73 F. Wu, M. Misra and A. K. Mohanty, *Prog. Polym. Sci.*, 2021, **117**, 101395.
74 S. Kaur, S. Sivasankaran, E. Wambolt and S. Jonnalagadda, *Int. J. Pharm.*, 2020, **573**, 118873.
75 A. Ghassemi, S. Moghaddamzadeh, C. Duchesne and D. Rodrigue, *J. Plast. Film Sheeting*, 2017, **33**, 361–383.

76 M. Imani, K. Dimic-Misic, M. Kostic, N. Barac, D. Janackovic, P. Uskokovic, A. Ivanovska, J. Lahti, E. Barcelo and P. Gane, *Sustainability*, 2022, **14**, 10425.
77 C. Pechyen and S. Ummartyotin, *Polym. Bull.*, 2017, **74**, 431–444.
78 S. Teixeira, R. Silva, T. De Oliveira, P. Stringheta, M. Pinto and N. de FF Soares, *Food Biosci.*, 2021, **42**, 101202.
79 L. K. Massey, in *Permeability Properties of Plastics and Elastomers*, ed. L. K. Massey, William Andrew Publishing, USA, 2nd edn, 2002, pp. 1–56.
80 A. Fajdek-Bieda and A. Wróblewska, *Polymers*, 2024, **16**, 2505.
81 A. Buzarovska, G. Bogoeva-Gaceva and R. Fajgar, *J. Polym. Eng.*, 2016, **36**, 181–188.
82 A. A. Shamsuri and Z. A. Sumadin, *Compos. Commun.*, 2018, **9**, 65–69.
83 I. Surya, E. Chong, H. A. Khalil, O. G. Funmilayo, C. Abdullah, N. S. Aprilia, N. Olaiya, T. Lai and A. Oyekanmi, *J. Mater. Res. Technol.*, 2021, **12**, 1673–1688.
84 E. G. Bajsić, V. Rek and B. O. Pavić, *J. Elastomers Plast.*, 2013, **45**, 501–522.
85 B. Lee, H. Kim, W.-B. Lee and Y.-M. Kim, *Environ. Eng. Res.*, 2024, **29**(3), 178–184.